J Mater Sci (2010) 45:4652–4658
DOI 10.1007/s10853-010-4382-y

ULTRAFINE GRAINED MATERIALS

Microstructure and tensile behavior of Al and Al-matrix carbon nanotube composites processed by high pressure torsion of the powders

Soo-Hyun Joo · Seung Chae Yoon · Chong Soo Lee · Dong Hoon Nam · Soon Hyung Hong · Hyong Seop Kim

Received: 12 February 2010 / Accepted: 3 March 2010 / Published online: 16 March 2010

Abstract Carbon nanotubes (CNTs) are expected to be ideal reinforcements of composite materials used in aircraft and sports industries due to their high modulus and low density. In the present paper, severe plastic deformation by high pressure torsion (HPT) of powders at elevated temperature (473 K) was employed to achieve both powder consolidation and grain refinement of aluminum-matrix nanocomposites reinforced by 5 vol% CNTs. Before the HPT, the powders were ball milled using planetary ball mill in order to achieve molecular level mixing. Aluminum was treated by the same process for a reference. The HPT processed disk were composed of considerably equilibrium grain boundaries with high misorientation angles. The CNT-reinforced ultrafine grained microstructural features resulted in high strength and good ductility.

Introduction

Recently, several methods of severe plastic deformation (SPD), i.e., large plastic straining under high hydrostatic pressure at low temperature, such as equal channel angular pressing (ECAP), high pressure torsion straining (HPT), accumulative roll bonding, etc., have been developed to bulk nano/ultrafine structured materials with a grain size from 20 to 200 nm [1]. Among the various SPD methods, the HPT process, a novel method for processing of nanostructured materials, has been investigated widely because of its ability to impose extremely high strain and hydrostatic pressure to develop homogeneous nanostructures with high angle grain boundaries (HAGBs) and high intrinsic stresses [2]. The HPT process can be applied not only for solid materials, but also for consolidation of powders to produce densely packed bulk materials [3, 4].

C60, fullerene and nanotubes, carbon nanotubes (CNTs) have attracted considerable research attention of scientific community due to their interesting properties caused by small size and unique structural diversities and large potential for practical applications [5]. For instance, mechanical properties of these materials differ significantly from the conventional materials. These materials may have a Young's modulus of 1 TPa and tense strength up to 30 GPa. The high modulus and the low density of CNTs make them ideal reinforcements in a variety of composite materials used in aircraft and sports industries. However, improvement of properties in metal-matrix systems are restricted because of the lack of uniform dispersion of CNTs in matrix and low interfacial bonding strength between the matrix and the CNT reinforcements [6]. Recently, several important works regarding novel synthetic processes and improved mechanical properties of CNT-reinforced metal-matrix (CNT/metal) nanocomposites have been reported [7, 8].

Recently, SPD processes have been successfully applied for uniform dispersions of CNT [9, 10] in metal matrix. Consolidation of the mixture of Al powders and CNTs was achieved by HPT at room temperature and a tensile strength more than 200 MPa was reported with reasonable

S.-H. Joo · C. S. Lee · H. S. Kim (✉)
Department of Materials Science and Engineering,
POSTECH (Pohang University of Science and Technology),
Pohang 790-784, Korea
e-mail: hskim@postech.ac.kr

S. C. Yoon
Automotive Steel Research & Development Team,
Hyundai HYSCO, Dangjin-gun 343-831, Korea

D. H. Nam · S. H. Hong
Department of Materials Science and Engineering, KAIST,
Daejeon 305-701, Korea

ductility [9]. However, effect of processing at elevated temperatures has not been reported. This study presents the processing of commercial pure Al powders with and without CNTs by HPT at elevated temperature (473 K). Microstructural features and tensile behavior of the HPT processed CNT-Al nanocomposites were investigated.

Experimental procedure

Preparation of powders and high pressure torsion process

Commercial pure aluminum powders and multi-wall CNTs with 10–40 nm in tube diameters were used to synthesize metal-matrix CNT nanocomposites by HPT at an elevated temperature (473 K). The HPT processing temperature was elevated in order to improve bonding of CNT/metal interface. The bottle necks in CNT/metal composites are interface bonding and homogeneous distribution of CNTs. Two novel methods: molecular-level mixing and HPT were employed. First, in order to enhance the interface bonding between the CNTs and metal matrix, a precursor of CNT/Cu nanocomposites was fabricated using a novel molecular-level mixing process before mechanical alloying with Al powders [7]. The molecular-level mixing treatment can be used to achieve good interface bonding between CNTs and metals as well as a homogeneous dispersion of CNTs in metal-matrix materials [11]. After molecular-level mixing treatment, the CNT/Cu powders of 5 vol% and Al powders of 95 vol% were treated by planetary ball milling. The Al powders with CNT/Cu nanocomposites were put into a 0.25-mm deep circular hole with 10 mm in diameter which was located at the center of the lower anvil as illustrated in Fig. 1. Then, the lower anvil went up until the mixture powders contacted the upper anvil having the same dimensions of the lower anvil. In the HPT step, 6 GPa pressure was applied for 10 s during compressive stage. Afterward, the lower anvil was rotated at a rotation speed of 1 rpm under the same constant pressure for 10 turns during torsional stage. For comparison, HPT were conducted on 0 and 5 vol% CNT/Cu nanocomposites with Al powders as well.

Evaluation of mechanical properties

For mechanical testing, surfaces of the HPT disks were ground with abrasive papers and polished up to 0.25 μm diamond powders. The prepared surfaces were observed by the field emission scanning electron microscopy (FE-SEM) using a JEOL JSM 6330F at 15 kV.

Vickers microhardness was measured from the center to the edge of the HPT disks using a Future-Tech FM-700 tester. The applied load and dwell time were 300 g and 10 s, respectively. For tensile testing, two dog bone-type specimens were cut from the HPT disks using a wire cutting machine. In the elongation region, a gauge length was 1.25 mm and width was 1.0 mm. The thicknesses of tensile specimens, 0.93 mm, were the same as that of the HPT processed disk. The tensile tests were performed at room temperature with an initial strain rate of 8.0×10^{-4} s^{-1}. During the tests, precise strains were measured by the vision strain gauge system (ARAMIS 5 M) which detects the 3D coordinates of the deforming object surface on the basis of digital image processing delivering also the 3D displacement and the strain.

The microstructural features with nano and submicro crystalline structures were investigated in terms of grain size, misorientation angle of grain boundaries, and their distributions. The surfaces of the HPT processed disks were ground with emery papers to 150 μm in thickness and fine polished with a fine cloth containing a suspension of diamond of 0.25 μm in diameter to obtain mirror-like surfaces. For electron backscattered diffraction (EBSD), 3 mm disks were cut at near the center of the sample, 2.5 and 5 mm away from the center using a mechanical punch. EBSD analysis was performed using a 3D Total Analysis (Dual FIB: Helios Nanolab) equipped with a field-emission gun (Hikari EBSD detector) at an accelerating voltage of 20 kV located in NCNT (National Center for Nano Technology) of POSTECH. Crystal orientations were determined by an automatic beam scanning with a step size of 20 nm on the measured area of 5.76×17.11 μm^2. The beam scanning step size of

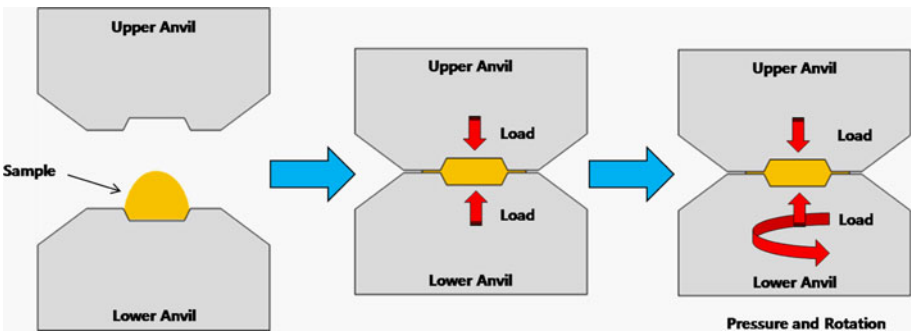

Fig. 1 Schematic illustration of HPT facility and operation with a pressure showing the first compressive stage and the next torsional stage

20 nm is the most accurate level, compared to the typical values of ~80 nm measured previously [12]. A cleaning up procedure was applied to all the EBSD images to adjust points with confidence index (CI) lower than 0.1. Misorientation angles <2° between two adjacent grains were excluded from the analyses, considering the limitations of the angular resolution of the EBSD technique [13]. For transmission electron microscopy (TEM), 3 mm disks were cut at a position 2.5 mm away from the center of the sample disk using a mechanical punch and the Focused Ion Beam (FIB) technique was used as a final step. Microstructures were observed using a JEOL JEM-2100F operation at 200 keV.

Results

The strain developed during HPT can be defined approximately as simple shear which can be given by the following equation: shear strain $\gamma = 2\pi rN/t$, where N is the rotation number, t is the height of the cylindrical specimen, and r is the distance from the torsion axis (i.e., disk center). In addition, the von Mises equivalent strain can be presented as $\varepsilon = \gamma/\sqrt{3}$. The shear strain and total equivalent strain introduced in HPT are 393 and 227, which are much larger than the strain values (5–10) introduced in the other SPD processes [14–16].

Figure 2 shows SEM images of the surface of the HPT processed Al powders sample with and without CNT/Cu reinforcements. The SEM image shows good densification without any residual pores. Good densification is obtained due to high hydrostatic pressure of 6 GPa which is much higher than the yield stress of the Al matrix. The grain sizes are too small to identify by typical etched SEM measurements, therefore, EBSD in FE-SEM and TEM were employed.

Vickers microhardness

Vickers microhardness of consolidated Al powder samples with and without CNT/Cu reinforcements are plotted as a function of distance from the center to the edge of the disk in Fig. 3. The Vickers microhardness of the Al-matrix sample without CNT/Cu reinforcements increased slightly from the center (70 Hv) to 1 mm away from the center (85 Hv). However, from 1 to 5 mm away from the center, no substantial increase in hardness was noticed. The hardness of the Al-matrix sample with CNT/Cu was found to be approximately two times greater than that without CNT/Cu reinforced sample and does not change remarkably with distance. It is considered that microstructures in both samples reached to steady state after 10 turns of HPT process at 473 K and therefore the hardness does not vary much with the distance. This finding of constant hardness values with distance from the center is consistent with the previous investigation in 99.99% pure Al performed by Harai et al. [17]. This constant hardness is attributed to the balance between the hardening due to an increase in dislocation density and the softening due to absorption of dislocation at high angle boundaries [18].

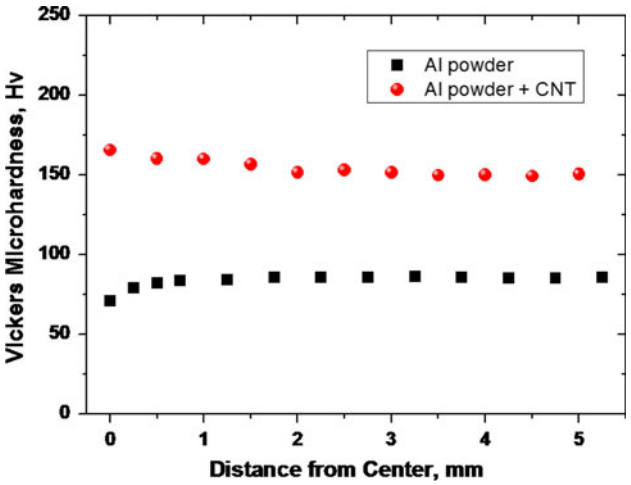

Fig. 3 Vickers microhardness of the compact disk of Al with and without CNTs/Cu from the disk center to edge after 10 turns of HPT under 6 GPa

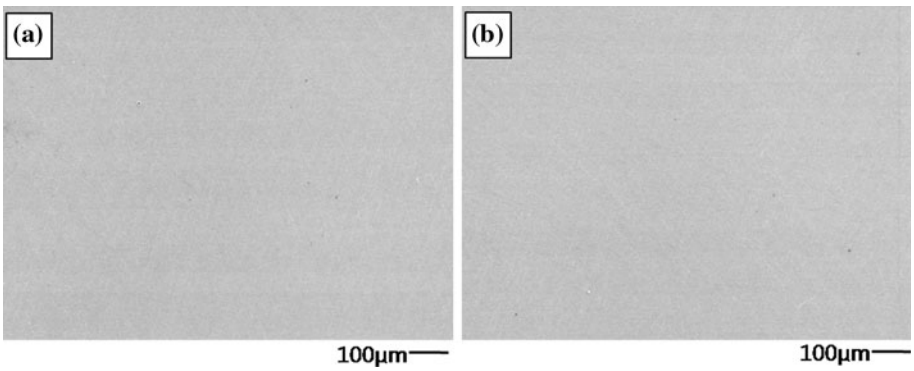

Fig. 2 SEM images of the HPT processed samples: **a** Al powders and **b** Al powders + CNT/Cu

EBSD

In order to demonstrate that the HPT processed discs (without CNT/Cu reinforcement) reach to steady state, microstructures of the HPT processed Al powders without CNT/Cu reinforcements were obtained at several positions along the radius obtained by EBSD (see Fig. 4). Microstructures observed by EBSD analysis at various positions along the radius confirms the presence of equiaxed and uniform nanocrystalline structures along the radius. Microstructure obtained at three positions, center, 2.5 mm from the center (middle of center and periphery) and 5 mm (periphery) away from the center were found to be similar. The average grain sizes at three positions are 290, 310, 295 nm, respectively. Normalized grain size distribution as presented in Fig. 5 indicates a uniform distributions of grain size at all points. The distributions of grain boundary misorientation angles are presented in Fig. 6 and the average misorientation angles are 21.7°, 20.7°, and 18.9°, which shows that considerable portions of HAGBs (misorientation angle >15°) were generated after the HPT process at 473 K.

TEM

Bright field and dark field images with selected area electron diffraction (SAED) patterns obtained from (a) Al and (b) Al +CNT/Cu consolidated discs are shown in Fig. 7. The average grain size of the Al samples without CNT/Cu is found to be ~300 nm whereas it is ~100 nm in the Al reinforced with CNT/Cu. The grain size of Al without CNT/Cu as measured by TEM is in good agreement with the grain size values obtained from the EBSD. The CNT/Cu reinforcements as indicated by the arrows, showed

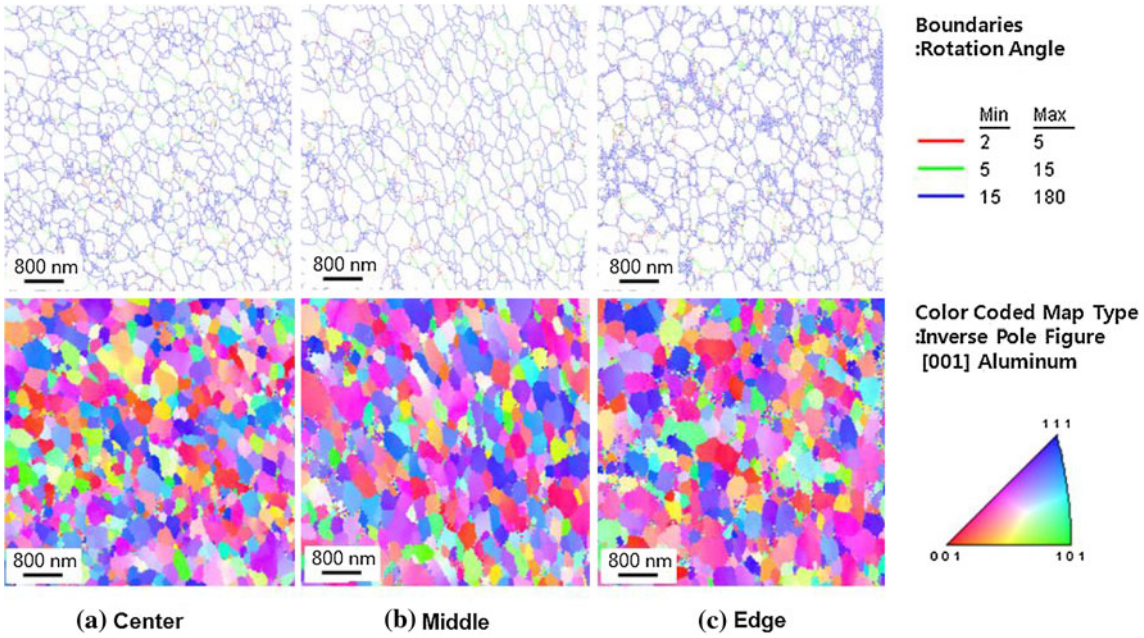

Fig. 4 Orientation images and image quality maps for the Al powder HPT sample. **a** Center, **b** middle, and **c** edge

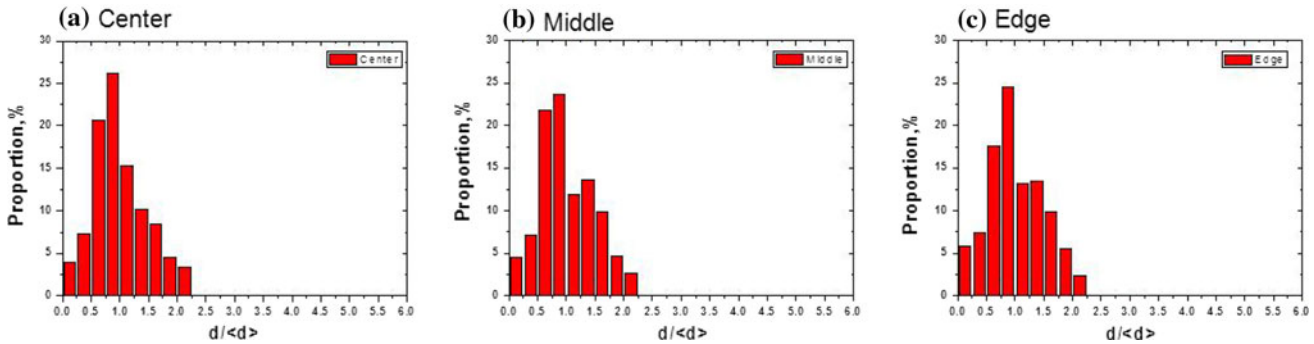

Fig. 5 The distribution of grain size. **a** Center, **b** middle, and (**c**) edge (d = grain size, and $\langle d \rangle$ = the average grain size)

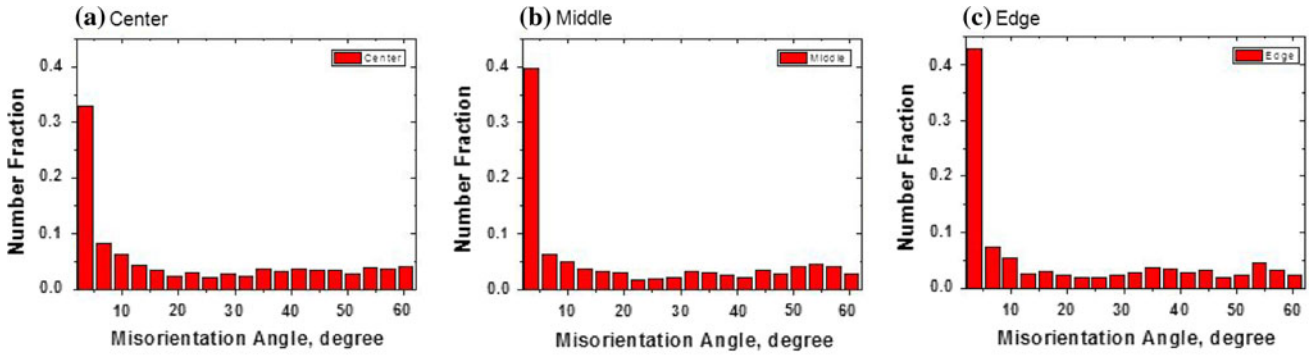

Fig. 6 Distribution of misorientation angle of the Al powder HPT sample in number fraction. **a** Center, **b** middle, and **c** edge

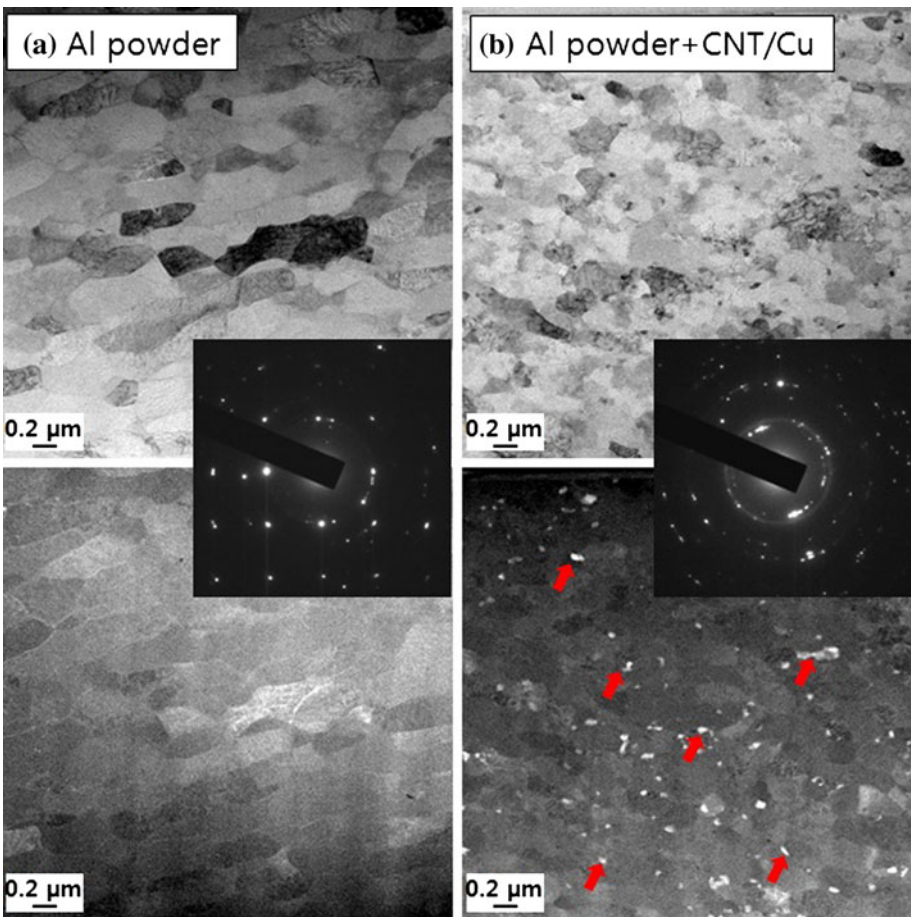

Fig. 7 Bright field and dark field images with SAED patterns obtained from **a** Al powders and **b** Al powders + CNT/Cu

uniform dispersion of CNTs in the matrix. Interestingly, majority of the CNT/Cu reinforcements are located at grain boundaries, which hinders the grain growth at elevated temperatures. After the HPT process at elevated temperature, the grain boundaries are in equilibrium states, as shown in the TEM images (Fig. 7). A large number of reflections with no azimuthal spreading in the SAED patterns are corroborative evidence of equilibrium grain boundaries.

Tensile tests

Tensile stress–strain curves of the HPT processed Al samples with and without CNT/Cu reinforcements are presented in Fig. 8. The HPT processed pure Al sample possesses an ultimate tensile strength of 255 MPa and 25% elongation failure. The tensile strength of Al composite with CNT/Cu reinforcements was found to be two times more than that without CNT/Cu reinforcements, show reasonably good

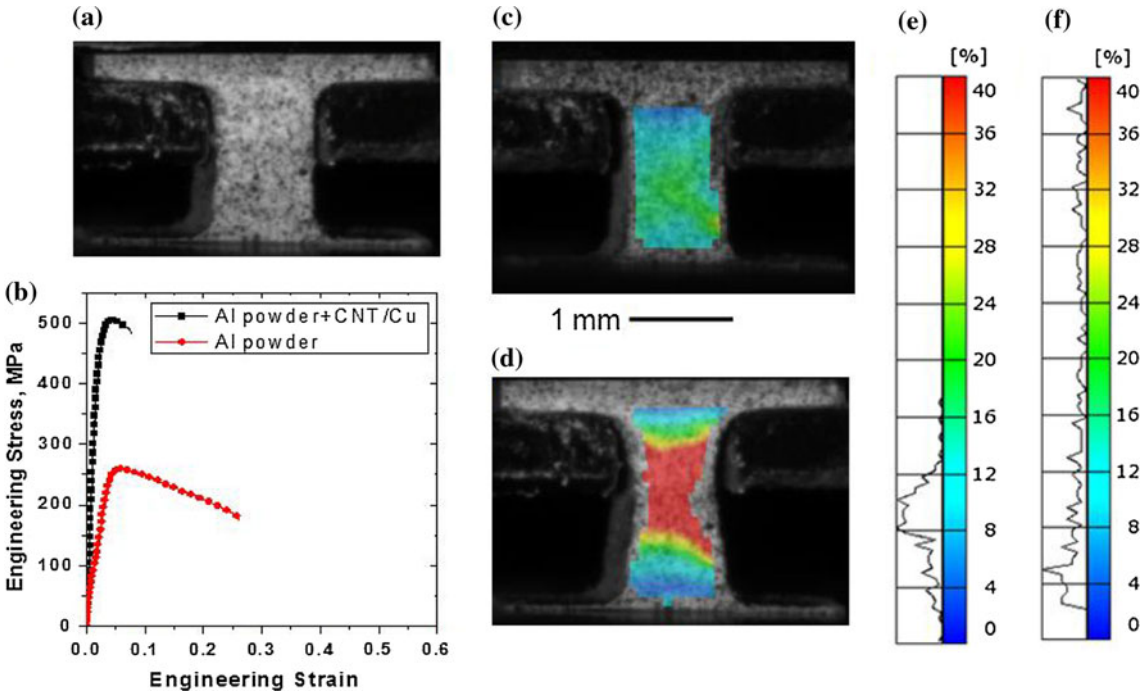

Fig. 8 Tensile test results. **a** Initial specimen image, **b** stress–strain curves, (**c**) major strain overlay of Al powder + CNT/Cu specimen, **d** major strain overlay of Al powder, **e** strain contour and distribution of Al powder + CNT/Cu and **f** strain contour and distribution of Al powder

ductility (9%). Hence, it can be concluded that the CNT/Cu reinforcements not only hinders the grain coarsening during the HPT process by pinning grain boundary motion, but also improves mechanical properties by providing obstacles to dislocation motion during plastic deformation.

Discussion

In this study, the Vickers microhardness and EBSD results reveal that the HPT disks of Al and Al-matrix CNT/Cu composites attain a steady-state condition, i.e., saturation of microstructural features and properties with strain, after 10 turns of HPT at 473 K. Since strain values developed in HPT is proportional to the number of rotations and distance from the center ($\gamma = 2\pi rN/t$), the effect of the other processing conditions, typically the number of turns, can be seen from the effect of distance from the center. Therefore, the similar microstructures in center, middle and edge can be an evidence for the steady state.

The grains are nearly equiaxed and homogeneous through the surface. The grain size after HPT processing was reduced to $\sim$300 nm in the Al (without CNTs) which is much smaller than in the other SPD processes as reported in literature. For example, grain size of commercial Al was reported to reduce from 0.9 μm after 12 passes of ECAE at 473 K [19] or 0.47 μm after 8 passes ECAE and annealing at 473 K for 1 h [20]. The previously reported samples are in the form of solid bulk. This trend of grain refinement by SPD is the same with the HPT processed Al powder at room temperature [9]. At elevated temperature, alumina particles on the initial Al powder surfaces cause dislocation accumulation and therefore further grain refinement. It should be noted that grain growth after or during SPD is the bottle neck for grain refinement, especially in pure metals. Indeed, in severely deformed commercial purity Al, abnormally grown grains appeared in specimens annealed at temperatures between 548 and 573 K [20]. However, in this study after the HPT process at 473 K, alumina particles reduce grain size, while abnormal grain growth is not detected during HPT. The absence of the abnormal grain growth is probably because (i) the sample was made from powder states which has many oxides which have a grain boundary pinning effect and (ii) the purity of the sample Al is not high, i.e., commercial purity. It should be noted that, on the other hand, Kawasaki et al. observed the abnormal grain growth in high purity Al during ECAP [21].

The microstructures of both samples with and without CNT/Cu have equilibrium boundaries and considerable grain boundaries are HAGBs with misorientation angle $>15°$. High plastic strains at room temperature produced the fragment boundaries which are rather nonequilibrium but, when heated, they are transformed into large-angle grain boundaries (equilibrium grain boundaries) [22]. Like annealing process, high-deformation processing at elevated temperature produces equilibrium boundaries with HAGBs.

These results are well explained by misorientation angle distributions obtained from EBSD observations. Grain boundary misorientation angles are significant characteristics of materials governing ductility [23] of SPD processed materials, i.e., ductility increases with increasing misorientation angle [24]. The good tensile properties are caused from this microstructural characteristics, i.e., fine grain size and HAGBs.

The TEM images of the sample with the CNT/Cu reinforcements show smaller grain size (100 nm). The CNT/Cu nano particles act as obstacles to dislocation glide and grain growth. Also, the nanocomposites are well dispersed in the matrix by the three steps: (i) molecular-level mixing, (ii) planetary ball milling with Al powders, and (iii) HPT processing. Another prominent role of dispersion of CNTs in the matrix is the enhancement of elastic properties of the Al/CNT composites [25]. Even though the process temperature is higher than room temperature, there is no aggregation of CNT/Cu reinforcements during the HPT process. Due to the above-mentioned reasons, the higher strength and Young's modulus in tensile tests are detected in the nanocomposites than in the Al samples without CNTs (see Fig. 8).

Conclusions

From HPT of powders employed at elevated temperature (473 K) to achieve both powder consolidation and grain refinement of aluminum-matrix nanocomposites reinforced by 5 vol% CNTs, we obtained the following conclusions.

I. Densification Al powders and dispersion of CNT/Cu were successfully achieved using HPT process at elevated temperature.
II. The HPT disks reached a steady-state condition and the grain sizes were reduced to 300 and 100 nm in case of Al without and Al with CNT, respectively, and achieved grain size is smaller than reported in case of bulk samples. Alumina particles and CNT/Cu nanocomposites prevented dislocation motion at elevated temperature.
III. The equilibrium grain boundaries were detected and considerable amount of them were HAGBs. This microstructural feature did an important role of high strength and good ductility.
IV. The well dispersed CNT/Cu nanocomposites effect on higher Young's modulus in tensile tests.

Acknowledgements This research was supported by Shinhan diamond Co. under the program of the Knowledge of Economy, Korea. Fruitful discussion with Dr. Gupta is appreciated. This research was supported by grants (code#: 08K1501-00510) from "Center for Nanostructured Materials Technology" under "21st Century Frontier R&D Programs," and "Priority Research Centers Program" through the National Research Foundation (NRF) funded by the Ministry of Education Science and Technology, Korea.

References

1. Valiev RZ, Islamgaliev RK, Alexandrov IV (2000) Prog Mater Sci 45:103
2. Zhilyaev AP, Langdon TG (2008) Prog Mater Sci 53:893
3. Alexandrov IV, Zhang K, Kilmametov AR, Lu K, Valiev RZ (1997) Mater Sci Eng A234:331
4. Stolyarov VV, Zhu YT, Lowe TC, Islamgaliev RK, Valiev RZ (2000) Mater Sci Eng A282:78
5. Popov VN (2004) Mater Sci Eng R43:61
6. Kuzumaki T, Miyazawa K, Ichinose H, Ito K (1998) J Mater Res 13:2445
7. Cha SI, Kim KT, Arshad SN, Mo CB, Hong SH (2005) Adv Mat 17:1377
8. Jeong YJ, Cha SI, Kim KT, Lee KH, Mo CB, Hong SH (2007) Small 3:840
9. Tokunaga T, Kaneko K, Horita Z (2008) Mater Sci Eng A490:300
10. Quang P, Jeong YG, Yoon SC, Hong SH, Kim HS (2007) J Mater Proc Tech 187–188:318
11. Kim KT, Cha SIl, Gemming T, Eckert J, Hong SH (2008) Small 4:1936
12. Gazder AA, Cao WQ, J CH. Davies, Pereloma EV (2008) Mater Sci Eng A497:341
13. Humphreys FJ (2004) Scripta Mater 51:771
14. Kim HS (2001) Mater Sci Eng A315:122
15. Moon BS, Kim HS, Hong SI (2002) Scripta Mater 46:131
16. Jang Y, Kim S, Han S, Lim C, Goto M (2008) Metal Mater Inter 14:171
17. Harai Y, Ito Y, Horita Z (2008) Scripta Mater 58:469
18. Ito Y, Horita Z (2009) Mater Sci Eng A503:32
19. Wang YY, Sun PL, Kao PW, Chang CP (2004) Scripta Mater 50:613
20. Yu CY, Sun PL, Kao PW, Chang CP (2004) Mater Sci Eng A366:310
21. Kawasaki M, Horita Z, Langdon TG (2009) Mater Sci Eng A524:143
22. Valiev RZ, Krasilnikov NA, Tsenev NK (1991) Mater Sci Eng A137:35
23. Kim HS, Estrin Y (2001) Appl Phys Lett 79:4115
24. Zhao YH, Topping T, Bingert JF, Thornton JJ, Dangelewicz AM, Li Y, Liu W, Zhu YT, Zhou YZ, Lavernia EL (2008) Adv Mater 20:3028
25. Lahiri D, Bakshi SR, Keshri AK, Liu Y, Agarwal A (2009) Mater Sci Eng A523:263